

## Electronic Structure of Aromatic Pseudohalides

Igor Novak\*

Department of Chemistry and CPEC Centre, National University of Singapore, Singapore 117543, Singapore

Branka Kovač

Physical Chemistry Division, "R. Bošković" Institute, HR-10000 Zagreb, Croatia

Received: March 7, 2002; In Final Form: January 15, 2003

The molecular and electronic structure of fourteen aromatic isocyanates and isothiocyanates has been investigated by HeI/HeII photoelectron spectroscopy, high-level DFT, and ab initio calculations, and their spectra have been compared with the spectra of related compounds.

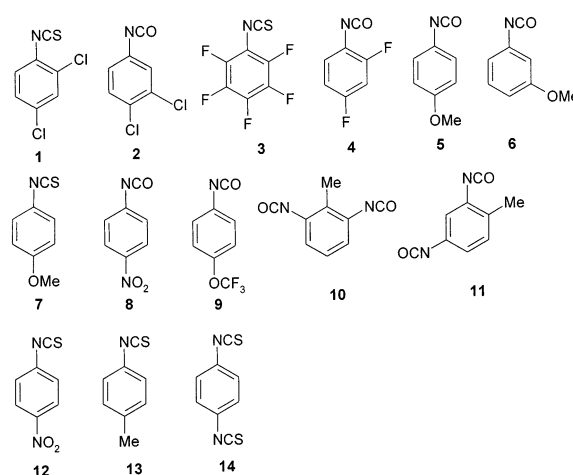
### Introduction

Aromatic pseudohalides (isocyanates and isothiocyanates) are interesting molecules for two reasons. First, aromatic isocyanates are important precursors in the synthesis of polymer materials. The production is based on nucleophilic addition reaction which takes place via the nucleophile's attack on the carbon of NCX group (X = O and S). The synthetic procedure gives high yields and exhibits no side reactions. Second, aromatic and alkyl pseudohalides are examples of distorted linear triatomic systems. The distortions from linearity of the NCX moiety have been investigated in some detail.<sup>1</sup> For aromatic pseudohalides, few gas phase structure measurements are available, and those that are do not describe the geometry of the NCX group accurately.<sup>2</sup> The electronic structure of pseudohalides is relevant for understanding their chemical behavior, so the compounds were investigated previously by UV photoelectron spectroscopy (UPS) and MO calculations. The derivatives studied were alkyl pseudohalides,<sup>3</sup> methyl pseudohalides,<sup>4</sup> silicon pseudohalides,<sup>5</sup> and halogen isocyanates.<sup>6</sup> Five aromatic pseudohalides have been included in the UPS/semiempirical MO study,<sup>3</sup> but no attempt was made to correlate their electronic structure with other properties (e.g., chemical reactivity). We therefore report the analysis of such relationships, including the discussion of intramolecular interactions between the aromatic ring and the NCX group, for a representative sample of aromatic pseudohalides.

### Experimental and Theoretical Methods

The compounds **1**–**14** were purchased from Fluka AG and used without further purification after checking their melting points.

The HeI/HeII photoelectron spectra of isocyanates and isothiocyanates **1**–**14** were recorded on the Vacuum Generators UV-G3 spectrometer and calibrated with small amounts of Xe gas which was added to the sample flow. The spectral resolution in HeI and HeII spectra was 25 and 70 meV, respectively, when measured as fwhm of <sup>2</sup>P<sub>3/2</sub> Ar<sup>+</sup> line. For compounds **1**, **2**, **7**, **10**, and **11**, the sample inlet temperature was 60 °C, for **3**–**6** and **9**, the temperature was 25 °C and for **8**, **12**, **13**, and **14**, the temperatures were 80, 80, 40, and 100 °C, respectively. These temperatures were necessary to obtain sufficient vapor pressures in the ionization region. The resolution of the HeII spectra was



always inferior to that of the HeI, which implies that some bands well-resolved in HeI become unresolved in the corresponding HeII spectrum. The consequence is that the measured relative band intensities and intensity ratios sometimes refer to a combined intensity of two bands rather than to a single band.

The quantum chemical calculations were performed with Gaussian 98 program.<sup>7</sup> The full geometry optimization was performed at DFT/B3PW91 level using TZ2P basis set. This level of calculation has been recently recommended for large molecules.<sup>8</sup> Subsequently, single-point calculations of ionization energies with the same basis set were performed by ROVGF method. The same optimized geometry was also used to perform natural population analysis (NPA). The ROVGF method goes beyond Koopmans approximation and is often used to interpret the photoelectron spectra.<sup>9</sup> The assignment of the spectra of large molecules can often be facilitated by measuring band intensities at various photon energies. The spectral bands (for the purposes of relative intensity measurements) were, when necessary, simulated by Gaussian profiles and baseline corrections were employed (Table 1). The empirical relative intensity RI(empir) for the *i*th band was calculated as

$$RI_i = \{B_i^{\text{HeI}} / \sum_i B_i^{\text{HeI}}\} / \{B_i^{\text{HeII}} / \sum_i B_i^{\text{HeII}}\}$$

where *B<sub>i</sub>* stands for the band intensity of the *i*th band in the HeI or HeII spectrum and the index of summation runs through

**TABLE 1: Vertical Ionization Energies ( $E_i \pm 0.05$  eV), Empirically and Theoretically Derived Band Assignments, Calculated Ionization Energies (GF/eV), and Ratios of Measured Band Intensities at HeII/HeI Radiation (RI)<sup>a,b</sup>**

compound	band	$E_i$	MO type	GF	RI
<b>1</b>	X	8.60	$\pi_b$	-8.40	2.0
	A-B	9.67	$\sigma_{\text{NCS}}, \pi_b$	-9.45, -9.64	1.6
	C	10.30	$\pi_{\text{NCS}}$	-10.22	1.4
	D-F	(11.61)	$\sigma_{\text{Cl}}, \pi_{\text{Cl}}, \sigma_{\text{Cl}}$	-11.61, -11.76, -11.84	0.5
	G-H	12.8	$\pi_{\text{Cl}}, \sigma$	-12.94, -13.13	
<b>2</b>	I-etc.	13.4	s	-13.91	
	X	9.00	$\pi_b$	-8.72	1.7
	A	9.68	$\pi_b$	-9.56	1.2
	B	(11.1)	$\pi_{\text{NCO}}$	-11.14	0.7*
	C-D	11.43	$\sigma_{\text{Cl}}, \sigma_{\text{NCO}}$	-11.3, -11.47	0.7*
	E	11.93	$\sigma_{\text{Cl}}$	-11.94	0.7*
	F	12.53	$\pi_{\text{Cl}}$	-12.44	
<b>3</b>	G	12.83	$\pi_{\text{Cl}}$	-13.03	
	X	9.2 (9.03)	$\pi_b + \pi_{\text{NCS}}$	-8.65	1.2
	A-B	10.13	$\pi_b, \sigma_{\text{NCS}}$	-9.56, -9.77	1.0
	C	(10.88)	$\pi_{\text{NCS}}$	-10.63	0.8
<b>4</b>	D	12.58	$\pi_b$	-12.60	1.6
	E	13.3	$\sigma_{\text{NCS}}$	-13.57	0.7
	X	9.08	$\pi_b$	-8.80	1.2
	A	10.05(9.9)	$\pi_b$	-9.80	0.9
	B	11.4	$\sigma_{\text{NCO}}$	-11.38	1.0*
<b>5</b>	C	11.7	$\pi_{\text{NCO}}$	-11.74	1.0*
	D	13.1	$\pi_b$	-13.41	
	X	8.28	$\pi_b$	-7.93	1.1
	A	9.58	$\pi_b$	-9.36	0.7
	B	10.58	$\pi_{\text{NCO}}$	-10.68	1.1*
	C	10.85	$\sigma_{\text{NCO}}$	-10.88	1.1*
	D	11.7	s	-12.01	
<b>6</b>	E	12.31	$\pi_b$	-12.42	
	F	12.85	s	-13.10	
	X	8.58	$\pi_b$	-8.30	1.1
	A	9.11	$\pi_b$	-8.74	1.0
	B-C	10.83	$\pi_{\text{NCO}}, \sigma_{\text{NCO}}$	-10.95, -10.95	1.0
<b>7</b>	D	11.85	s	-12.09	
	E	12.13	p	-12.32	
	X	8.10	$\pi_b$	-7.77	1.3
	A-C	9.63	$\sigma_{\text{NCS}}, \pi_b, \pi_{\text{NCS}}$	-9.0, -9.5, -9.56	0.9
<b>8</b>	D	11.23	$\pi_b + \pi_{\text{NCS}}$	-11.67	
	E	11.75	$\sigma_{\text{OMe}}$	-12.06	
	X	9.56	$\pi_b$	-9.30	0.8
	A	10.28	$\pi_b$	-10.12	0.8
	B-C	11.27	$\pi_{\text{NO}_2}, \sigma_{\text{NO}_2}$	-11.15, -11.33	1.1
	D-E	11.27	$\sigma_{\text{NCO}}, \pi_{\text{NCO}}$	-11.48, -11.53	1.1
<b>9</b>	F	12.13	$\pi_b + \pi_{\text{NCO}}$	-12.13	1.1
	X	9.14	$\pi_b$	-8.76	1.4
	A	10.07	$\pi_b$	-9.70	0.8
	B-C	11.63	$\sigma_{\text{NCO}}, \pi_b + \pi_{\text{NCO}}$	-11.24, -11.62	1.1
	D	12.3	s	-12.24	0.7
<b>10</b>	X-A	9.07	$\pi_b, \pi_b$	-8.44, -8.68	1.4
	B-D	11.11	$\pi_{\text{NCO}}, \sigma_{\text{NCO}}, \sigma_{\text{NCO}}$	-10.96, -10.99, -11.06	1.3
	E	12.38	$\pi_{\text{NCO}}$	-12.32	0.7
	F	12.78	s	-13.04	0.7
<b>11</b>	X	8.73	$\pi_b$	-8.30	1.0
	A	9.26	$\pi_b$	-8.93	1.0
	B-D	10.8611.06	$\pi_{\text{NCO}}, \sigma_{\text{NCO}}, \sigma_{\text{NCO}}$	-10.86, -10.96, -11.16	1.0
	E	12.25	$\pi_{\text{NCO}}$	-12.27	
	F-G	12.61	$\sigma, \sigma$	-12.99, -13.01	
<b>12</b>	X	9.08	$\pi_{\text{NCS}}$	-8.82	0.9
	A	9.9	$\sigma_{\text{NCS}}$	-9.71	0.8*
	B	10.25	$\pi_b$	-10.18	0.8*
	C	10.9	$\pi_b$	-10.77	1.1*
	D-F	11.1	$\pi_{\text{NO}_2}, \sigma_{\text{NO}_2}, \sigma_{\text{NO}_2}$	-11.21, -11.31, -11.54	1.1*
	G-H	12.75	$\sigma, \pi_b$	-13.10, -13.18	
	X	(8.28)	$\pi_b$	-8.06	1.3
<b>13</b>	A-B	9.48	$\sigma_{\text{NCS}}, \pi_b$	-9.05, -9.42	1.0
	C	10.0	$\pi_{\text{NCS}}$	-9.87	0.9
	D-E	11.9	$\pi_b + \pi_{\text{NCS}}, \sigma$	-12.25, -12.28	
	X	8.43 (8.23)	$\pi_b$	-8.06	1.3
<b>14</b>	A-C	9.6	$\pi_{\text{NCS}}, \sigma_{\text{NCS}}, \sigma_{\text{NCS}}$	-9.37, -9.40, -9.42	1.0
	D	9.9	$\pi_b$	-9.93	1.0
	E	(10.76)	$\pi_{\text{NCS}}$	-10.74	0.8
	F-G	12.33	$\pi_b, \sigma$	-12.71, -12.75	

<sup>a</sup> Average RI values for bands which could be resolved in HeI, but not in HeII spectra; adiabatic ionization energies are given in brackets and have uncertainty of 0.03 eV. <sup>b</sup> The bands were simulated by asymmetric Gaussian band shapes as suggested in ref 17, and the variable bandwidths were in the range 0.1–0.3 eV.

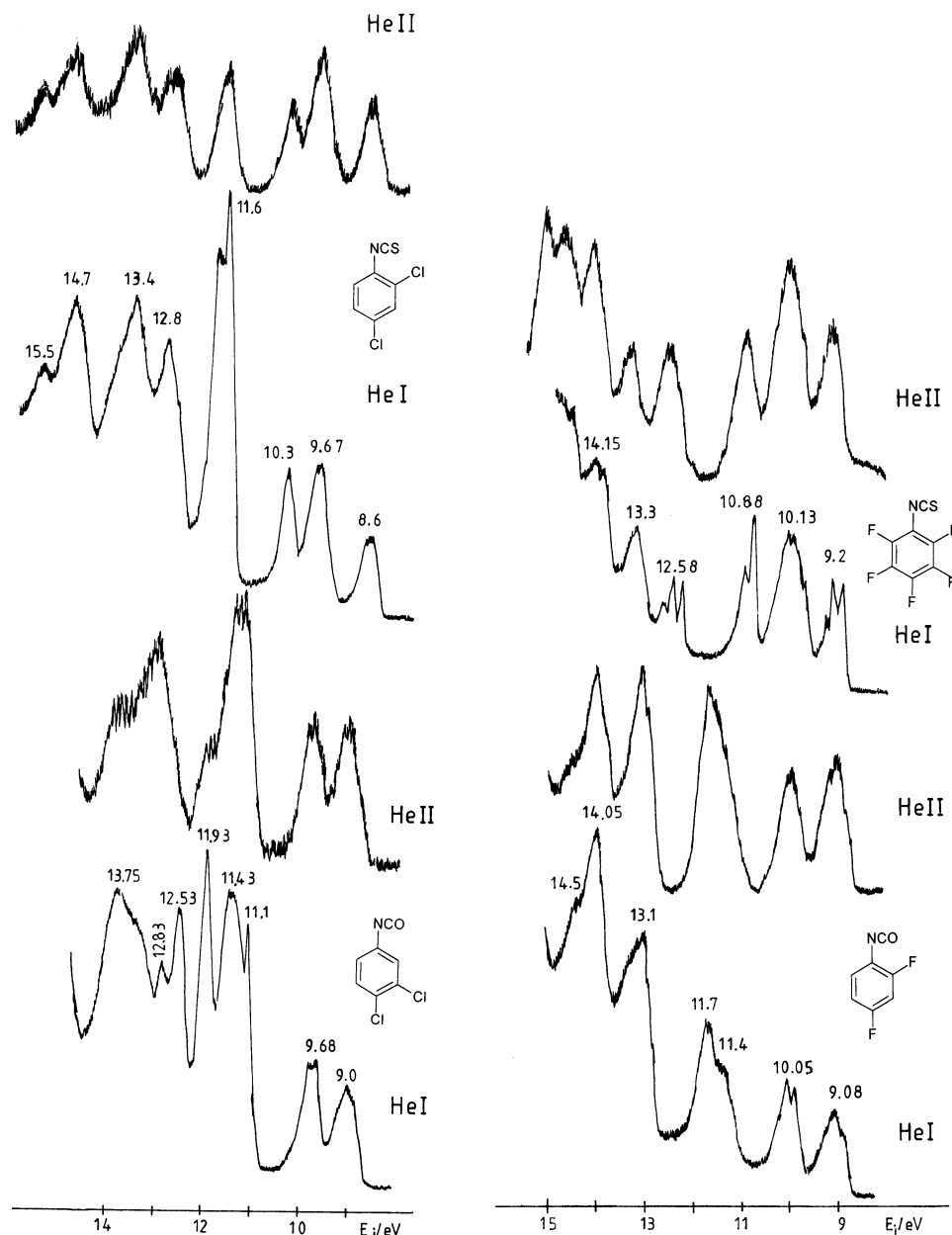


Figure 1. HeI/HeII photoelectron spectra of 1–4.

the bands of interest. In our case the bands of interest were ring  $\pi$ -ionizations and NCX group orbitals. RI value is the ratio of the intensity of a particular band (in HeI or HeII spectrum) normalized by the total intensity for the group of bands. The normalization is necessary, because absolute band intensities could not be measured.

## Results and Discussion

**(A) Electronic Structure.** The analysis of the photoelectron spectra (Figures 1–4) is summarized in Table 1. Figures indicate that the density of ionic states is large and one must combine several empirical and theoretical arguments in order to obtain reliable assignments.

The empirical arguments used in the assignment were based on the following considerations:

the bands observed in the 8–13 eV region correspond to ionizations from the ring  $\pi$ -orbitals ( $\pi_b$ ), the out-of-plane orbitals on NCX group ( $\pi_{\text{NCX}}$ ), in-plane orbitals of NCX group ( $\sigma_{\text{NCX}}$ ), chlorine lone pairs ( $\pi_{\text{Cl}}$ ,  $\sigma_{\text{Cl}}$ ), and  $\text{NO}_2$  group localized orbitals ( $\pi_{\text{NO}_2}$ ,  $\sigma_{\text{NO}_2}$ ).

These orbitals are expected to appear in the 8–13 eV region as the comparison with the spectra of related molecules—alkyl pseudohalides,<sup>4</sup> halobenzenes,<sup>10,11</sup> methoxy benzenes<sup>12</sup> and nitrobenzene—demonstrates. The bands with energies > 13 eV, overlap strongly in the spectra due to the high density of ionic states and cannot be reliably assigned. They will not be discussed further in this work.

The relative intensity of bands (RI) can be calculated from the comparison of relative band intensities in HeI and HeII spectra. The intensity changes reflect photon energy dependence of atomic photoionization cross-sections for various orbitals. The cross-section ratios for C2p, O2p, N2p, S3p, F2p, and Cl3p orbitals on going from HeI to HeII radiation are 0.31, 0.64, 0.45, 0.14, 0.90, and 0.05, respectively.<sup>13</sup> The ratios indicate that fluorine and chlorine localized orbitals (lone pairs) should exhibit strong and distinct variations in band intensities and consequently be readily identifiable in the spectra. However, fluorine lone pairs have high ionization energies (17 eV) and can be found in the region of high ionic state density. The cross-section of S3p orbital experiences the second smallest cross-

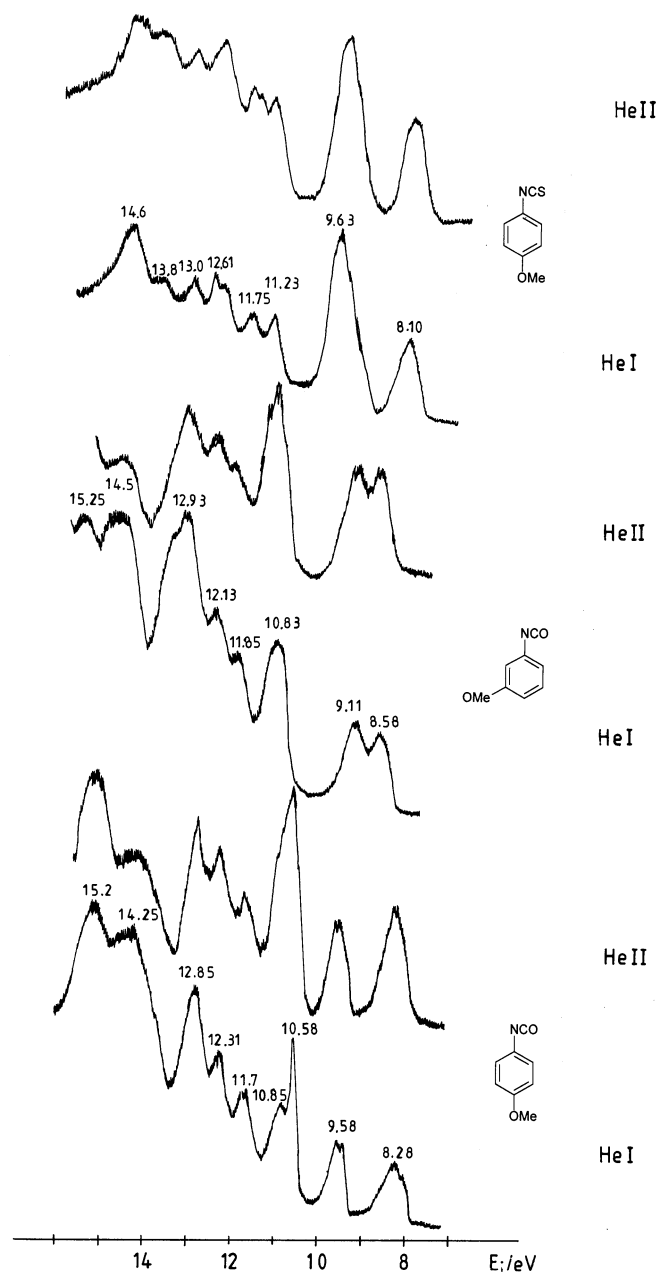


Figure 2. HeI/HeII photoelectron spectra of 5–7.

section ratio and therefore molecular orbitals with S3p character should also be identifiable in the spectra. Unfortunately, the cross-section ratios for C2p, N2p, and O2p orbitals do not differ sufficiently to permit unambiguous band assignments, so other arguments must be used instead. Furthermore, overlap between bands containing ionizations from MOs with different character reduces the size of observed HeI/HeII band intensity variations. These comments are borne out by the measured relative intensities (Table 1) which thus vary within the narrow range.

The sharp, narrow bands correspond to the ionization from strongly localized, nonbonding orbitals as suggested by the Franck–Condon principle.

Composite molecule method was used when comparing the UPS of structurally related molecules i.e., those containing the same functional groups. The method was employed when other empirical arguments could not provide definitive assignments.

The important information about aromatic pseudohalides concerns the interaction between ring  $\pi$ -orbitals and NCX group. On energy grounds, it can be expected that NCX- $\pi$  delocaliza-

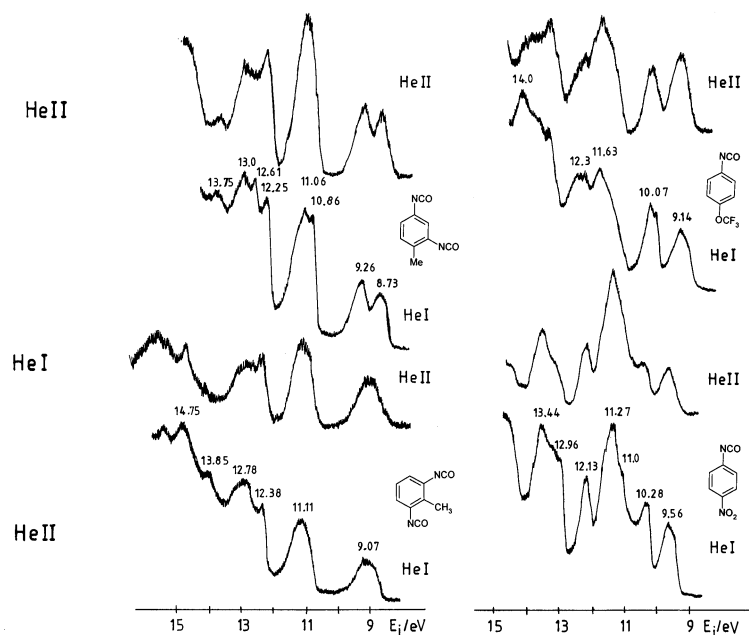


Figure 3. HeI/HeII photoelectron spectra of 8–11.

tion/interaction shall be more prominent in isothiocyanates than in isocyanates. This is due to a lower energy gap between NCS and ring  $\pi$ -orbitals compared to NCO vs ring  $\pi$ -orbitals. Further indication of stronger interaction in isothiocyanates comes from the comparison of UPS of alkyl-isothiocyanates<sup>3</sup> with their aromatic analogues (this work). In alkyl derivatives, the relevant NCS bands are sharper than in aromatic ones, which support the notion of stronger orbital mixing/interaction in the latter.

Specific assignment details for each class of molecules are given in the paragraphs below.

**Halogenated Derivatives (1–4).** The spectra of 1–4 (Figure 1) were analyzed with respect to the criteria mentioned above. The final assignment is given in Table 1. The bands in the spectra of 1–4 exhibit the expected energy level shift toward higher ionization energies (Figures 5 and 6), due to the electron withdrawing halogen substituents. In 3, the existence of “per-fluoro effect” is reflected in stronger stabilization of  $\sigma$  vs  $\pi$  orbitals. As a consequence of this effect, even the lowest lying  $\pi_b$  orbital could be detected (at 12.58 eV). The chlorine lone pair bands are easily recognizable by their strong HeI/HeII intensity variation.

**Methoxy Derivatives (5–7).** The spectra of 5–7 (Figure 2) contain fewer bands than their halogen analogues 1–4. Bands in 5–7 can be assigned on the basis of comparison with UPS of MeNCX<sup>4</sup> and methoxy benzene.<sup>12</sup> The reduction in the number of bands (i.e. quasi degeneracy of NCX bands) is an indication that the electron donating methoxy substituent reduces NCX–Ph interactions which is then followed by the reduction of measured splitting between  $\sigma_{\text{NCX}}$  and  $\pi_{\text{NCX}}$  orbitals. A shift toward lower ionization energy (compared to halogenated derivatives 1–4) is also noticeable in 5–7 and can be expected to arise when electron-donating methoxy substituent is present.

**Methyl, Nitro and Miscellaneous Derivatives (8–14).** Three molecules in this class 10, 11, and 14 have two identical NCX groups and the natural question arises concerning the efficiency of benzene ring as a vehicle for NCX–NCX intramolecular, through-bond interactions. Judging by the existence of clusters of nearly degenerate  $\sigma_{\text{NCX}}$  and  $\pi_{\text{NCX}}$  bands, the aromatic system appears not to be very efficient in this role. The compounds 8 and 12 are nitro derivatives and the NO<sub>2</sub> group orbitals can be identified by comparison with UPS of other nitro compounds.<sup>14</sup>

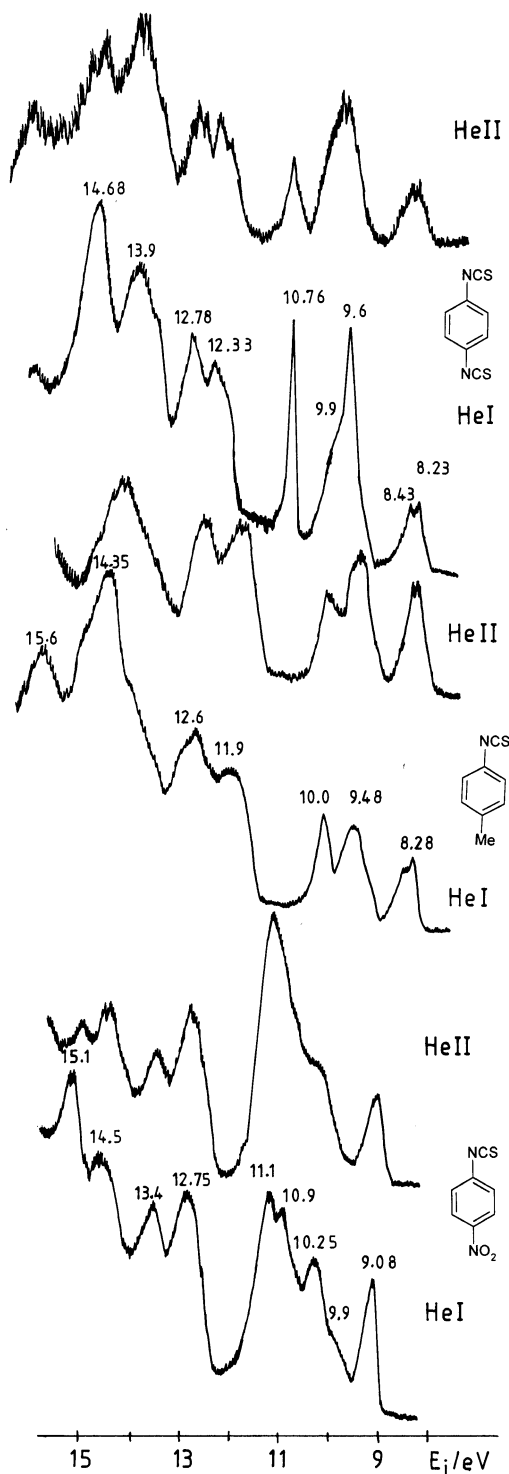


Figure 4. HeI/HeII photoelectron spectra of 12–14.

The interesting detail is that HOMO and SHOMO in **12** have pronounced NCS character, unlike in other molecules where the two topmost orbitals have more ring  $\pi$ -character (Figures 5–6).

**(B) Molecular Structure and Chemical Reactivity.** The geometrical parameters calculated for NCX group are given in Table 2. The accuracy of the DFT method used was tested by calculating geometries for HNCX molecules for which accurate experimental data are available.<sup>1</sup> Our method gives bond angles which deviate by  $<1^\circ$  and  $<0.006 \text{ \AA}$  from the experimental values (Table 2). Although MW spectroscopic studies of some aromatic pseudohalides had been reported,<sup>2</sup> the structure

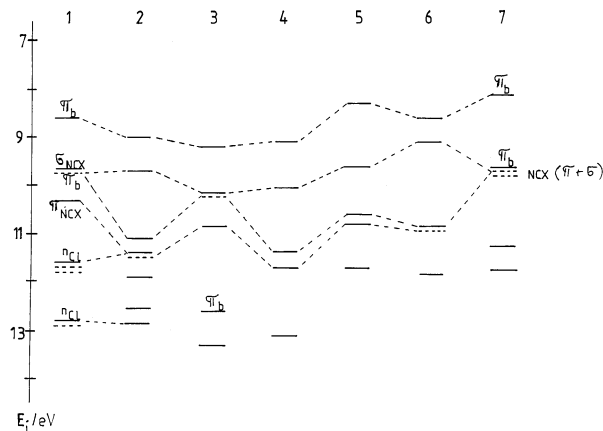


Figure 5. Energy level diagram of 1–7.

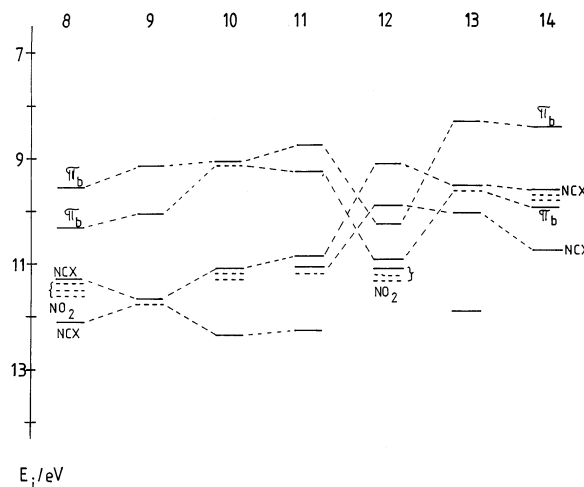


Figure 6. Energy level diagram of 8–14.

TABLE 2: Geometrical Parameters of Aromatic Pseudohalides Ph–CNX (X = O and S) Obtained by DFT Calculations at B3PW91/TZ2P Level

molecule	NC bond/ $\text{\AA}$	C–X bond/ $\text{\AA}$	$\angle\text{CNC}/\text{deg}$	$\angle\text{CNX}/\text{deg}$
<b>1</b>	1.190	1.574	150.8	176.2
<b>2</b>	1.210	1.165	138.8	173.5
<b>3</b>	1.197	1.567	145.8	174.8
<b>4</b>	1.201	1.166	139.4	173.8
<b>5</b>	1.201	1.169	139.8	173.6
<b>6</b>	1.202	1.167	138.9	173.5
<b>7</b>	1.186	1.582	153.6	176.5
<b>8</b>	1.205	1.164	138.3	173.4
<b>9</b>	1.203	1.166	138.8	173.5
<b>10</b>	1.202	1.167	139.0	173.7
<b>11</b>	1.202	1.166	139.1	173.5
<b>12</b>	1.192	1.572	149.5	175.8
<b>13</b>	1.186	1.580	153.5	176.4
<b>14</b>	1.190	1.576	150.8	176.1
HNCO (exptl)	1.214	1.166	123.9 (<HNC)	172.6 (<NCO)
HNCO (DFT)	1.211	1.163	123.3	172.2
HNCS (exptl)	1.207	1.567	131.7 (<HNC)	173.8 (<NCS)
HNCS (DFT)	1.200	1.571	131.9	174

determinations used assumed values for NCX geometry parameters. Inspection of Table 2 reveals that the influence of ring substituents on the NCX group geometry is generally small, especially when it comes to bond lengths. The only discernible influence concerns bond angles in NCS group and follows the trend according to which the electron-withdrawing/donating substituents lead to decrease/increase of  $\angle\text{CNC}$  angles.

The results of natural population analysis show that the average partial atomic charges ( $\pm 0.01$ ) in the NCO group are

for C, +0.86; for N, -0.54; and for O, -0.47 and in the NCS group, for C, +0.24; for N, -0.43; and for S, 0.0 ( $\pm 0.05$ ). Once again, like in the case of geometry parameters, various ring substituents do not significantly affect electron density of NCX groups. The chemical reactivity of the NCX group is based on the nucleophilic attack on the electron deficient carbon which can be rationalized by simple resonance structures:  $\text{R}-\text{N}=\text{C}=\text{O} \leftrightarrow \text{R}-\text{N}^--\text{C}^+=\text{O} \leftrightarrow \text{R}-\text{N}=\text{C}^+-\text{O}^-$

This is in accordance with our population analysis, which shows that NCX carbon always has a positive partial charge. However, since in isocyanates the carbon's partial charge is considerably larger, they can be expected to be more reactive than their isothiocyanate analogues. The overall conclusion is that the ring substitution does not influence the geometry or density of NCX to any significant extent.

### Summary

The energy and electron density of the topmost occupied molecular orbitals of aromatic pseudohalides had been analyzed and this may have further implications for the understanding of their chemical reactivity.<sup>15</sup> This is because the most reactive pseudohalide forms the most stable carbanionic intermediate in which nucleophile is bound to the electron deficient NCX carbon.<sup>16</sup> The ionization energy of the least stable NCX localized orbital may be an indicator of chemical reactivity; the higher the ionization energy (the lower the NCX orbital energy), the more stable the intermediate shall be.

### References and Notes

- (1) Rozsondai, B. In *The Chemistry of Sulphur-containing Functional Groups, Supplement S*; Patai, S., Rappoport, Z., Eds.; J. Wiley: Chichester, 1993; p 110.
- (2) *Landolt-Bernstein New Series II/15*; Springer: Berlin 1987; p 539. *Landolt-Bernstein New Series II/21*; Springer: Berlin 1992; p 395.
- (3) Neijzen, B. J. M.; De Lange, C. A. *J. Electron Spectrosc. Relat. Phenom.* **1980**, *18*, 179.
- (4) Pasinszki, T.; Veszpremi, T.; Feher, M.; Kovač, B.; Klasinc, L.; McGlynn, S. P. *Int. J. Quantum Chem., Quantum Chem. Symp.* **1992**, *26*, 443.
- (5) Veszpremi, T.; Pasinszki, T.; Feher, M. *J. Chem. Soc., Faraday Trans.* **1991**, *87*, 3805.
- (6) Frost, D. C.; Macdonald, C. B.; McDowell, C. A.; Westwood, N. P. C. *Chem. Phys.* **1980**, *47*, 111.
- (7) Frisch, M. J.; Trucks, G. W.; Schlegel, H. B.; Scuseria, G. E.; Robb, M. A.; Cheeseman, J. R.; Zakrzewski, V. G.; Montgomery, J. A., Jr.; Stratmann, R. E.; Burant, J. C.; Dapprich, S.; Millam, J. M.; Daniels, A. D.; Kudin, K. N.; Strain, M. C.; Farkas, O.; Tomasi, J.; Barone, V.; Cossi, M.; Cammi, R.; Mennucci, B.; Pomelli, C.; Adamo, C.; Clifford, S.; Ochterski, J.; Petersson, G. A.; Ayala, P. Y.; Cui, Q.; Morokuma, K.; Malick, D. K.; Rabuck, A. D.; Raghavachari, K.; Foresman, J. B.; Cioslowski, J.; Ortiz, J. V.; Stefanov, B. B.; Liu, G.; Liashenko, A.; Piskorz, P.; Komaromi, I.; Gomperts, R.; Martin, R. L.; Fox, D. J.; Keith, T.; Al-Laham, M. A.; Peng, C. Y.; Nanayakkara, A.; Gonzalez, C.; Challacombe, M.; Gill, P. M. W.; Johnson, B.; Chen, W.; Wong, M. W.; Andres, J. L.; Gonzalez, C.; Head-Gordon, M.; Replogle, E. S.; Pople, J. A. *Gaussian 98*, revision A.11; Gaussian, Inc.: Pittsburgh, PA, 1998.
- (8) Pascal, R. A. *J. Phys. Chem. A* **2001**, *105*, 9040.
- (9) Potts, A. W.; Trofimov, A. B.; Schirmer, J.; Holland, D. M. P.; Karlsson, L. *Chem. Phys.* **2001**, *271*, 337.
- (10) Bieri, G.; Åsbrink, L.; von Niessen, W. *J. Electron Spectrosc. Relat. Phenom.* **1981**, *23*, 281.
- (11) (a) Ruščić, B.; Klasinc, L.; Wolf, A.; Knop, J. V. *J. Phys. Chem.* **1980**, *85*, 1486; (b) *J. Phys. Chem.* **1980**, *85*, 1490; (c) *J. Phys. Chem.* **1980**, *85*, 1495.
- (12) Friege, H.; Klessinger, M. *Chem. Ber.* **1979**, *112*, 1614.
- (13) Yeh, J. J. *Atomic Calculation of Photoionization Cross-sections and Asymmetry Parameters*; Gordon and Breach: Langhorne, 1993.
- (14) Mok, C. Y.; Chin, W. S.; Huang, H. H. *J. Electron Spectrosc. Relat. Phenom.* **1991**, *57*, 213.
- (15) Ulrich, H. *Chemistry and Technology of Isocyanates*; Wiley: New York 1996.
- (16) Carroll, F. A. *Perspectives on Structure and Mechanism in Organic Chemistry*; Brooks/Cole: Pacific Grove, 1998.
- (17) Lichtenberger, D. L.; Copenhaver, A. S. *J. Electron Spectrosc. Relat. Phenom.* **1990**, *50*, 335.